energies

MDPI

Article

Effects of Tip Speed Ratios on the Blade Forces of a Small H-Darrieus Wind Turbine

Sajid Ali [1,2] and Choon-Man Jang [1,2,*]

[1] Department of Civil & Environmental Engineering, University of Science & Technology (UST), 217, Gajeong-ro, Yuseong-gu, Daejeon 34113, Korea; sajid_ali@kict.re.kr
[2] Department of Land, Water and Environmental Research, Korea Institute of Civil Engineering and Building Technology (KICT), Daehwa-dong 283, Goyangdae-ro, Ilsanseo-gu, Goyang-si 10223, Korea
* Correspondence: jangcm@kict.re.kr; Tel.: +82-31-910-0494

Abstract: Lift force is an important parameter for the performance evaluation of an H-Darrieus wind turbine. The rotational direction of the streamlined force is effective on the performance of the wind turbine. In order to analyze the flow characteristics around the turbine blades in real-time, a numerical analysis using three-dimensional unsteady Reynold-averaged Navier–Stokes equations has been introduced. Experimental data were obtained from a field test facility constructed on an island in South Korea and was introduced to compare the numerical simulation results with measured data. The optimum tip speed ratio (TSR) was investigated via a multi-variable optimization approach and was determined to be 3.5 for the NACA 0015 blade profile. The turbine displays better performance with the maximum power coefficient at the optimum TSR. It is due to the delay in the flow separation from the blade surface and the relatively lower strength of the tip vortices. Furthermore, the ratio between lift and drag forces is also the highest at the optimum TSR, as most of the aerodynamic force is directly converted into lift force. For one rotation of the turbine blade at the optimum TSR, the first quarter of motion produces the highest lift as the static pressure difference is maximum at the leading edge, which helps to generate maximum lift. At a TSR less than the optimum TSR, small-lift generation is dominant, whereas at a higher TSR, large drag production is observed. Both of these lead to lower performance of the turbine. Apart from the TSR, the optimum wind angle of attack is also investigated, and the results are prepared against each TSR.

Keywords: H-Darrieus wind turbine; blade force; tip speed ratio; internal flow analysis; lift force; drag force

Citation: Ali, S.; Jang, C.-M. Effects of Tip Speed Ratios on the Blade Forces of a Small H-Darrieus Wind Turbine. *Energies* **2021**, *14*, 4025. https://doi.org/10.3390/en14134025

Academic Editor: Andrés Elías Feijóo Lorenzo

Received: 12 June 2021
Accepted: 1 July 2021
Published: 4 July 2021

1. Introduction

Wind turbines can be divided into horizontal axis and vertical axis wind turbines according to the installation direction of the turbine blades. A horizontal axis wind turbine (HAWT) is generally preferred for large-scale electricity production because of its higher efficiency and greater power generation potential. A vertical axis wind turbine (VAWT) is mainly used in small-scale sites close to living environments such as the rooftops of residential buildings. The Straight-bladed H-Darrieus wind turbine is a type of VAWT. The rotor blades of the H-Darrieus VAWT are continuously affected by the angle of attack corresponding to the changing wind direction, which cause difficulty in understanding the complex internal flow of the turbine. Recently, research papers on wind turbines have been published with improved numerical analysis models and computing power enhancements.

Howell et al. [1] carried out numerical simulations of the H-Darrieus turbine to evaluate the impact of blade surface roughness on aerodynamic performance. They mentioned that the smoother the blade surface of the wind turbine is, the more likely flow separation from the blade surface is, thereby reducing the power that is generated. Claessens [2] analyzed the effect of blade thickness and the Reynolds number on the aerodynamic performance of the VAWT. The author stated that a thin blade could easily cut the incoming

air, separating the flow from the blade surface; therefore, the blades could experience a dynamic stall during rotation. Thick blades can also negatively affect the performance when blades act as a blunt body, which increases the drag force. Sabaeifard et al. [3] examined the effects of several design parameters, including the number of blades, airfoil type, and solidity, on the performance of VAWTs through transient simulations. They stated that NACA 0018 performs better in terms of continuity in power generation at low values of tip speed ratios due to the relatively lower strength of the tip vortices. Ponta et al. [4] designed a novel blade for Darrieus rotors and carried out numerical simulations to compare the turbine efficiency with the traditional H-Darrieus rotors. The power production with the novel blade was much smoother than the conventional one due to the improvements in the turbine starting characteristics at low TSRs. Yu et al. [5] investigated the effect of turbulence intensity and reduced the frequency of free-stream wind on dynamic stalls with a fixed value Reynolds number. They reported that the wind angle of attack was delayed as the reduced frequency increased. They also concluded that, as the turbulence intensity increases from 0.5 to 6.9%, stall angles can be further delayed at the constant Reynolds number of 4500. Mohamed [6] modified the blade shape of the H-Darrieus rotor for small residential applications, such as rooftops, using numerical simulations. The author mentioned that the turbine performance was directly related to the mutual aerodynamic interaction between all the blades, and this interaction largely depends on the wakes formed behind each of the blades and turbine solidity. Castelli and Benini [7] examined the effects of blade shape and airfoil thickness on flow separation and the aerodynamics of H-Darrieus rotors using a 2D CFD model. They showed that a vortex is formed at the tip, but the traveling of the vortex alongside the blade's surface is different depending on the blade's shape.

The wind angle of attack of an H-Darrieus rotor is one of the important parameters that impact the turbine's performance. As the rotor is continuously rotating, the angle of attack changes with every azimuthal position, making it difficult to understand the aerodynamic performance. Until now, there has been a limited number of studies that address these challenges. For instance, Joo et al. [8] studied the aerodynamic effect of the wind angle of attack on the performance of a two-bladed H-Darrieus wind turbine rotor as compared to a three-bladed rotor. They reported that the two-bladed rotor produces more tip vortices and wake regions, while the angle of attack is reduced due to the reduced solidity of the two-bladed rotor. Gupta and Biswas [9] studied the impact of the wind angle of attack on the aerodynamic performance of a three twist-bladed H-Darrieus wind turbine. They tried to design a blade by making it twisted in order to optimize the dynamically changing wind angle of attack as the blades rotate. They reported that lift and drag forces increased with the increase in the wind angle of attack. Patil et al. [10] performed a large eddy simulation to determine the values of the wind angle of attack at fixed azimuthal positions for a straight-bladed H-Darrieus wind turbine operating at a constant TSR and Reynolds number. They found that flow separates from the lower surface of the blade more rapidly than the upper surface when the wind angle of attack increases. They also reported that pitch angle is an important parameter, as all blades should interact with the incoming wind at an optimum angle of attack. Paraschivoiu et al. [11] suggested a theoretical model to control the pitch angle of H-Darrieus wind turbine blades to optimize the wind angle of attack. The authors claimed that annual energy production could be increased by optimizing the wind angle of attack via a pitch control strategy. As the study was purely theoretical, there was no discussion regarding the internal flow conditions and wind-blade interaction phenomenon. Gosselin et al. [12] conducted a parametric study to investigate the effects of the wind angle of attack using three conditions of TSRs during one complete rotor rotation. They found that lower TSRs produce more drag and wakes that enlarge the angle of attack and, therefore, reduce the power coefficient. In the case of very large TSRs, other negative phenomena, such as dynamic stalls and low-lift generation, lowers the overall aerodynamic performance. That is why they suggested a mid-range TSR in order to make sure the wind angle of attack is neither too large nor too small.

Many researchers have also studied the impact of different geometrical parameters on the performance of the VAWT. Li et al. [13] stated that an increase in turbine solidity helps reduce the static pressure on blade surfaces. Consul et al. [14] mentioned that the power coefficient increases as the number of blades increases to four from two. Chen et al. [15] discovered that the optimum amplitude of sinusoidal pitching variation ranges from five to ten degrees. Amstrong et al. [16] performed numerical simulations on straight-bladed VAWTs at a high Reynolds number. They mentioned that the wind turbines have peak power production capabilities during the first quarter of their rotation at a high Reynolds number.

The lift and drag forces, which change in time with the turbine rotor rotation, are important performance parameters of the H-Darrieus rotor. The basic understanding of the forces is still limited, and few previous studies can be found in the literature. Most researchers investigated the effects of geometrical parameters and blade shape on the performance of the VAWT. Therefore, it is important to understand the basic distribution of lift and drag forces with tip speed ratios according to azimuthal positions.

In the present study, the effects of the angle of attack on the lift and drag forces with tip speed ratio are analyzed for the blade profile NACA 0015 of an H-Darrieus wind turbine using numerical simulations and experimental measurements. The optimum pitch angle with respect to the azimuthal angles is also determined for one complete rotation of the turbine rotor. The data obtained through numerical simulations are compared with the results of the experimental measurements.

This paper conducts a differentiated study on the H-Darrieus wind turbine. Firstly, many aerodynamic variables have been optimized in a novel stepwise approach. The optimum values of the angle of attack and lift and drag coefficients have been determined for one rotation. Then, these optimized values are used as inputs to optimize other parameters, i.e., TSR and pitch angle. All the variables are optimized for every azimuthal position. This multi-variable and multi-layer optimization make a unique and applicable combination to be followed by other researchers conducting similar studies.

The contents of the paper are described as follows. Section 1 provides a comprehensive literature review of studies conducted recently on the aerodynamic performance of H-Darrieus wind turbines. Research gaps are identified at the end of this section, and the present study's purpose is mentioned. Section 2 covers the materials and methods used in the present study. Section 2.1 provides essential details about the numerical model, computational domain, boundary conditions, grid system, and analysis techniques. Section 2.2 is about the experimental methodology adopted. Section 3 contains the results and discussion, in which Section 3.1 has the results of the numerical model validation/comparison with the experimental data. Section 3.2 is the main section that explains the important findings and explains them physically with the help of numerical simulations. Finally, Section 4 is the conclusions of the present study. A list of variables and abbreviations used in this study is included at the end of this section.

2. Methods of Numerical Simulation and Experimental Measurements

2.1. Numerical Methods

Numerical analysis was performed using commercial software, SC/Tetra (Ver. 12, MSC Software, Seoul, Korea). Figure 1 shows the computational domain. In the figure, 'D' is the rotational diameter of the turbine rotor. The wind turbine was placed at a distance of 7.5 D right of the domain inlet; 20 D left of the domain outlet, whereas the front width of the domain was approximately 15 D (blockage ratio 6.66%). The computational domain was selected to ensure that wakes behind the rotor and other unsteady aerodynamic phenomena could be studied and captured accurately.

Boundary conditions were also declared accordingly. Blades are stated as wall; a vertical surface on the left of the domain is an inlet (velocity); similarly, the vertical surface on the right of the domain is an outlet (pressure). Symmetric condition is applied at the both sides of the domain. The bottom wall is stationary, whereas the upper and side walls

are declared as slip walls. Velocity at the inlet was 5 m/s, and pressure at the outlet was set as the atmospheric pressure.

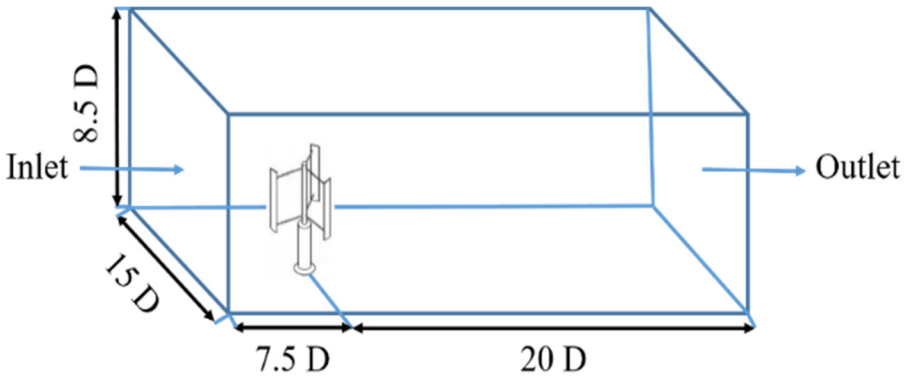

Figure 1. Computational domain for numerical simulation.

Table 1 summarizes the geometric features of an H-Darrieus rotor.

Table 1. Geometry of the turbine rotor.

Parameter	Value
Blade profile	NACA 0015
Rotational diameter (D)	2 m
Blade height (H)	3 m
Chord length (c)	0.2 m
Turbine solidity (S)	0.1

An H-type three-bladed VAWT was introduced in the present study. It has a blade height of 3 m, a rotational diameter of 2 m (sweep area of 6 m^2), a solidity of 0.1, and a NACA0015 airfoil, with a chord of 0.2 m. The wind turbine has a smooth shaft with a circular cross-section with a radius of 0.01 m, which has the same rotational speed and direction as the wind turbine. Figure 2 shows the geometric details of the wind turbine in the present study.

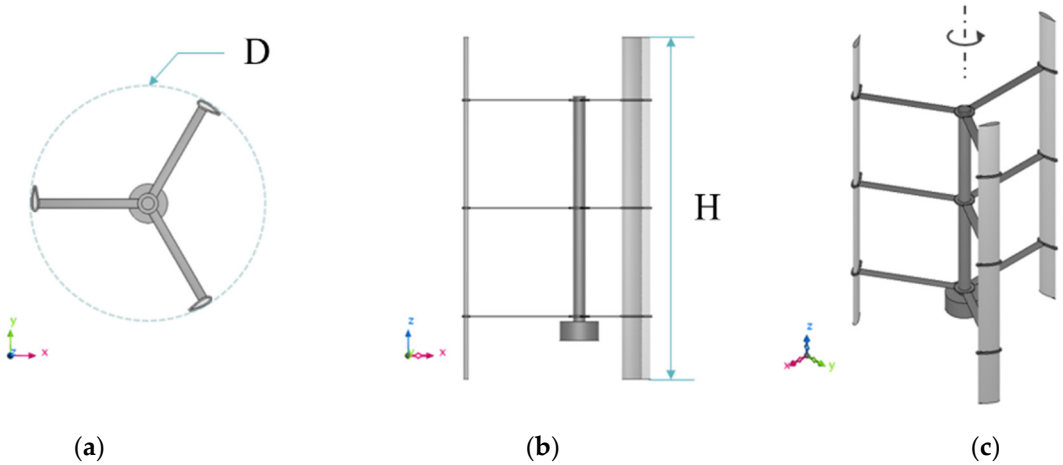

Figure 2. Detail view of the H-Darrieus rotor (**a**) rotational diameter (**b**) blade height (**c**) perspective view [17].

Figure 3 shows the computational grid around the turbine blade.

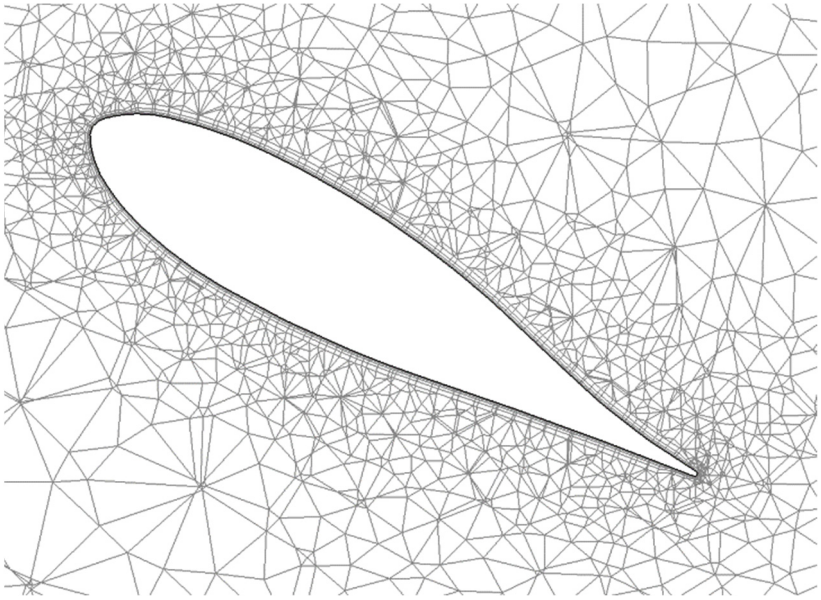

Figure 3. Computational grid around a turbine blade [17].

An unstructured grid was created for all blades by utilizing the advanced built-in mesh sizing functions in SC/Tetra. In order to capture the complex flow phenomenon around the blades, 5 layers of inflation were introduced at the blade surface, having an expansion rate of 1.2. Apart from the regions near the blades, the remainder of the domains were primarily meshed using tetrahedral and prism elements.

In order to determine the optimum number of computational grids, a grid-dependency test was conducted and 1,600,000 was selected as the optimum number of grids for the computational domain, as shown in Figure 4.

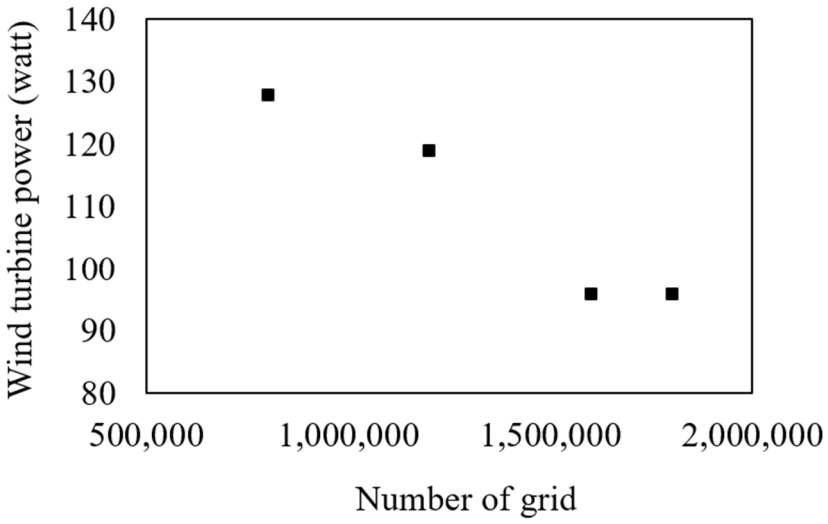

Figure 4. Grid independency test result [17].

Table 2 shows the grid settings adopted in present study. Mostly, tetrahedral mesh elements are used for capturing the high turbulence downstream of wind turbine. Different number of prism layers have been applied for turbine blades and all other stationary walls. Five prism layers have been utilized for blades in order to model the highly turbulent phenomena whereas three prism layers near the stationary walls will allow to decrease the computational time.

Table 2. Meshing details.

Parameter	Value
Mesh type	tetrahedral and prism
Number of total elements	1,600,000
Number of prism layers (Turbine)	5
Number of prism layers (Wall)	3

The accurate selection of the time-step for transient analysis is one of the key challenges as the flow conditions continuously alter as the turbine rotates. In the present study, the time-step was selected by adopting the Courant number (*CN*), which has the following mathematical expression for the transient simulation time-step (*dt*) [17]:

$$CN = \frac{udt}{dx} \quad (1)$$

where u is the velocity and dx is the grid spacing. Generally, it is preferred to set the value of the Courant number as low as possible (<1) for transient and complex fluid flows. However, by doing so, the time-step size would be very small, which increases the computational cost and time for each numerical simulation. Therefore, an intermediate value of the Courant number was chosen in the present study, as mentioned in Table 3. The increment of the azimuthal position ($d\theta$) was kept at 0.1° for more detailed and accurate calculations of unsteady simulations.

Table 3. Time-step selection.

TSR (-)	*CN* (-)	$d\theta/dt$ (°/s)	dt (s)
1	2.68	0.1	0.00035
2	1.88	0.1	0.000176
3	1.43	0.1	0.000115
4	1.37	0.1	0.000088
5	1.37	0.1	0.00008

In the present study, unsteady calculations were performed using a large eddy simulation (LES). To analyze the complex unsteady phenomenon such as interaction of wake with the rotating blades, a 2nd-order upwind spatial discretization algorithm was utilized. For transient calculations, a 2nd-order implicit formulation was employed. It is known for minimizing the interpolation errors in the numerical diffusion. Smagorinsky's eddy viscosity model with the damping function of Van Driest used for the LES has already been described in a paper published by authors [18]. If the residuals of all the flow variables are less than 10^{-5}, it is considered a converged solution. The turbulence intensity in the free-stream wind at the inlet of the computational domain is 5%.

In order to consider the fluctuations occurring during the starting of the wind turbine, the values of instantaneous torque and power coefficients were recorded for at least three cycles. After that, the data become more stable, and therefore, the present simulation used the results obtained after three complete rotations of the rotor.

2.2. Experimental Method of a Darrieus Wind Turbine

A Darrieus wind turbine, having the same geometrical dimensions as the model for numerical simulation, was fabricated and installed on the Deokjeok-do island, South Korea, as shown in Figure 5.

The wind turbine power is proportional to the cubic power of the wind speed. Wind speed with time was measured using a cup-anemometer installed on the met-mast, as shown in Figure 5. The wind speed data were measured and stored for one full year, 2016. Figure 6 shows the power curve of the wind turbine.

Figure 5. Wind turbine at experimental site

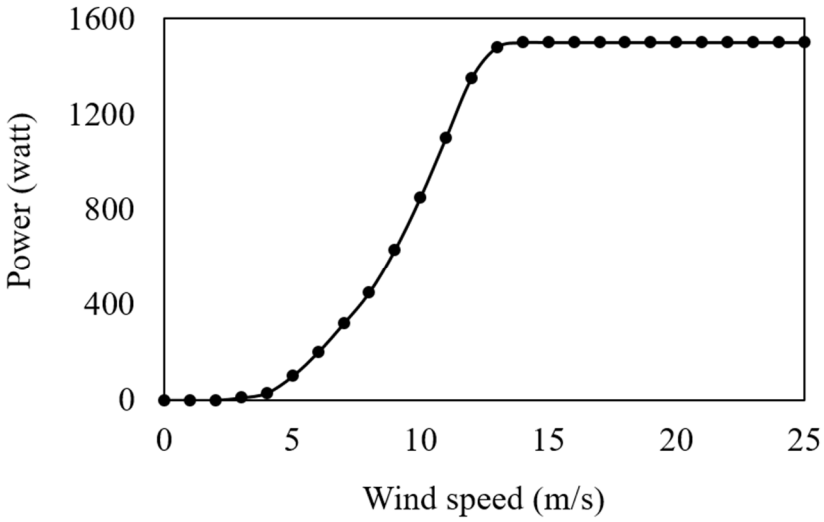

Figure 6. Power curve of wind turbine installed at experimental site [17].

3. Results and Discussion

3.1. Validation of Numerical Model with Experimental Data

To validate the numerical simulations, the power production of the H-Darrieus wind turbine is compared to the experimental data at different wind speeds, as shown in Figure 7. This image shows that the power computed using a numerical solution matches well with the experimental data. It is noted that there is only an 8% maximum difference in the values. It should be mentioned that the wind turbine power was slightly over-predicted by the numerical simulation at all wind speeds. Throughout the validation of the numerical results against the experimental results for the wind turbine performance, it can be concluded that the wind turbine power is being simulated accurately in the present study.

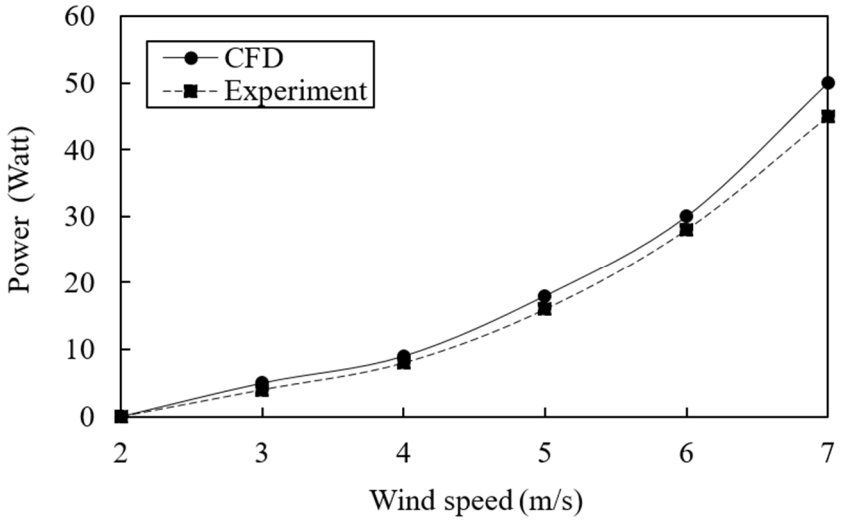

Figure 7. Comparison between numerical simulation and experimental results.

3.2. Effect of TSR on the Distribution of Aerodynamic Forces

The lift coefficient (C_L) and the drag coefficient (C_D) are the most important parameters related to the aerodynamics of wind turbines. Ideally, the ratio of the lift coefficient to the drag coefficient (C_L/C_D) should be maximized at all wind angles of attack (α).

Figure 8 shows the lift to drag coefficient ratio according to the angle of attack (α) at all the TSRs (λ) tested in the present study. It is noted that the range of α represents one complete rotation of a single blade.

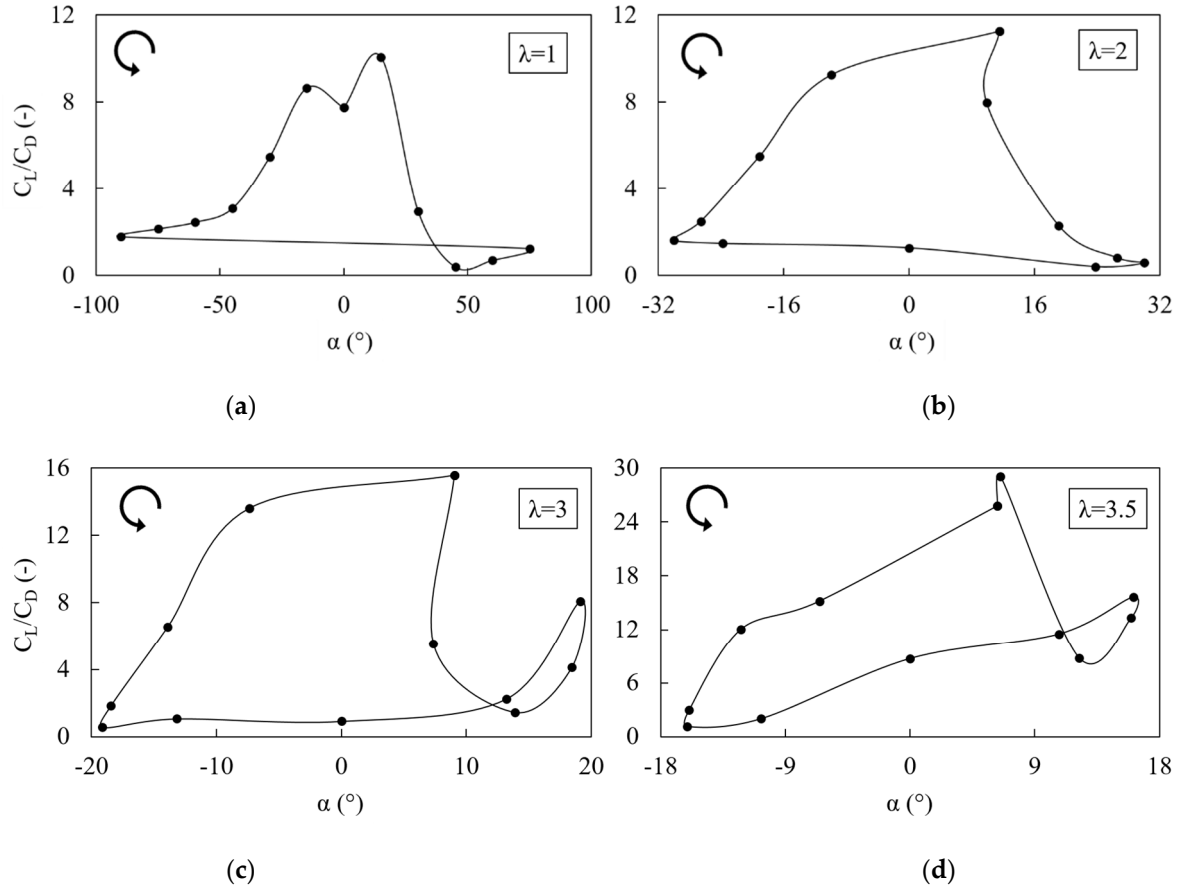

Figure 8. *Cont.*

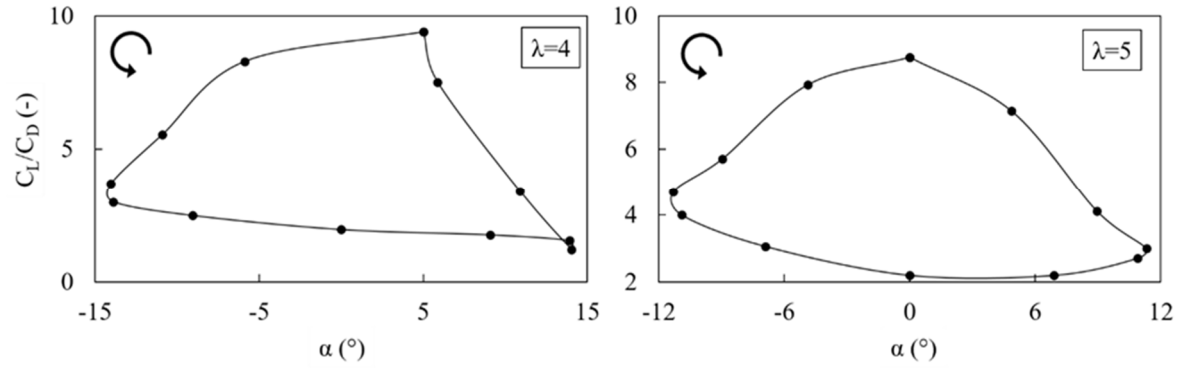

Figure 8. C_L/C_D for single blade for one turbine blade rotation: (**a**) TSR = 1, (**b**) TSR = 2, (**c**) TSR = 3, (**d**) TSR = 3.5, (**e**) TSR = 4, (**f**) TSR = 5.

In Figure 8, two distinct patterns are observed. One is that the range of α narrows as λ increases from 1 to 5. This is because, as the blade rotates at a higher speed, the relative velocity of the wind over the blade increases, which makes α go down (as α is essentially the angle between the relative wind speed and the blade tangential velocity). Secondly, the ratio of the C_L/C_D is one of the most critical parameters related to the airfoil aerodynamics. With an increase in λ from 1 to 3.5, the peak of C_L/C_D reaches a maximum of almost 30, and then reduces to 9 as λ is further increased to 5. One possible reason for this behavior is that as λ increases, drag increases rapidly, as shown in Figure 9.

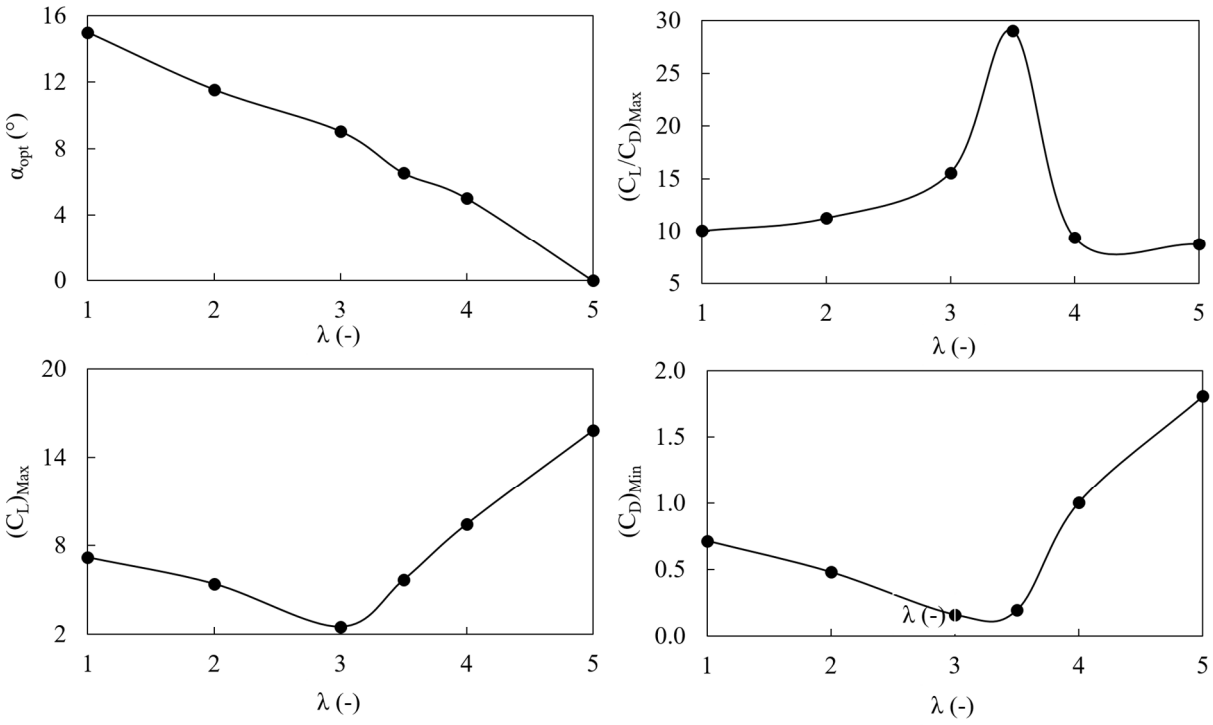

Figure 9. Optimized values of aerodynamic parameters for all TSRs.

Figure 9 shows the optimized aerodynamic parameters with respect to λ. Actually, C_L/C_D was optimized first, and then the remaining parameters were estimated. λ = 3.5 is the best scenario in the present study for NACA 0015, as C_L/C_D reaches a maximum value of 30. Although the C_L is maximized at λ = 5, C_D is also at its highest magnitude; therefore, it impacts the C_L/C_D ratio, and the value is reduced. As the figure shows the

optimized values of important aerodynamic parameters, it is also important to find the optimal angle of attack (α_{opt}) at which all these parameters have maximum values. Figure 9 shows the α_{opt} against each TSR considered in this study. At this value of α_{opt}, C_L/C_D will be maximized against the corresponding TSR. The value of α_{opt} decreases linearly with the TSR, due to an increased momentum of wind with which it strikes the blade surface [17].

Figure 10 shows the pressure and shear stress on a single blade for one turbine rotor rotation at all the TSRs. Aerodynamic pressure is responsible for lift generation, whereas shear stress on blade surface produces drag.

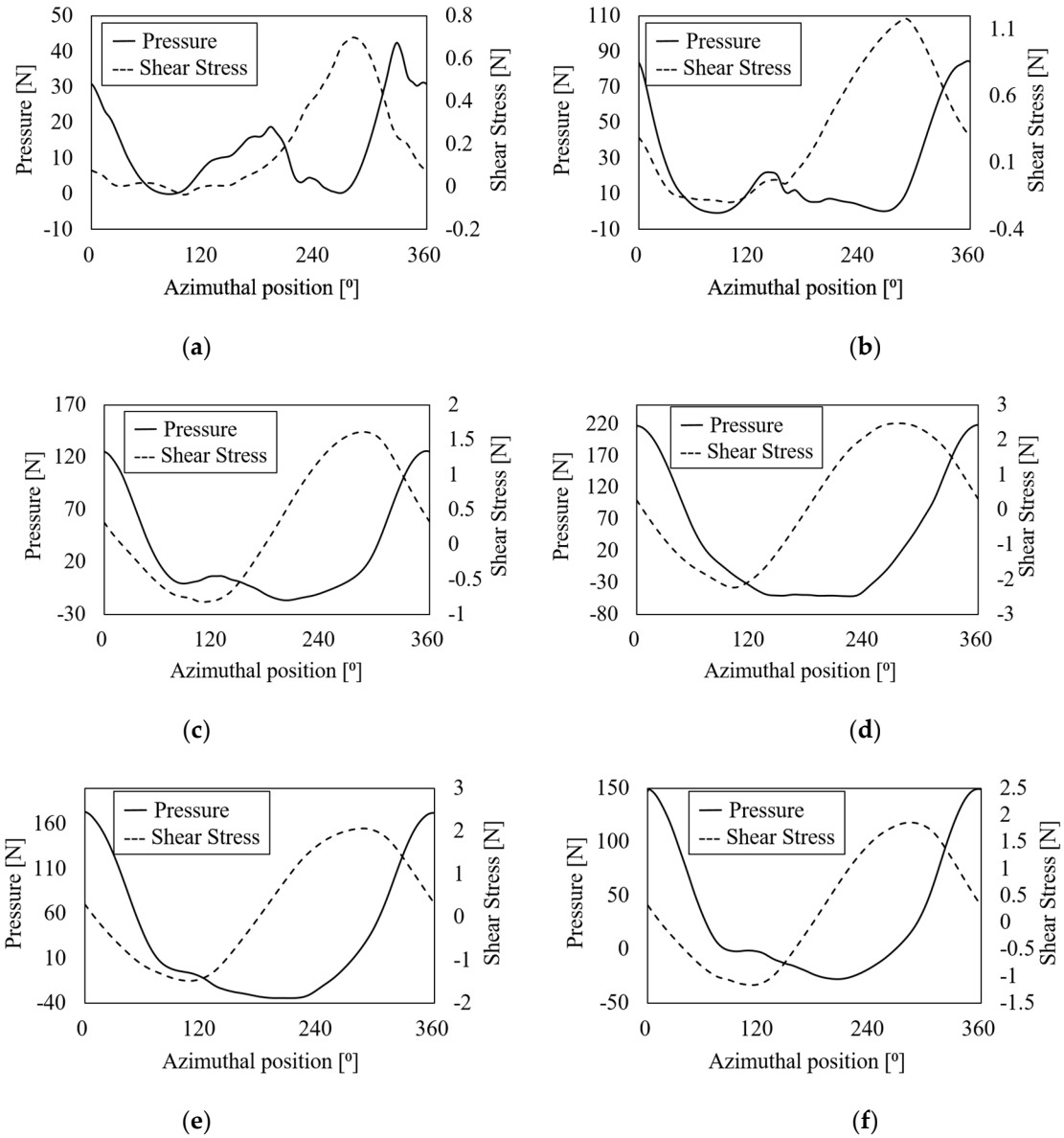

Figure 10. Pressure and shear stress for one turbine rotor rotation: (**a**) TSR = 1, (**b**) TSR = 2, (**c**) TSR = 3, (**d**) TSR = 3.5, (**e**) TSR = 4, (**f**) TSR = 5.

At lower TSRs, the fluctuations in forces are high, which produces unsteady torque and vibrations in the blades and other parts of a wind turbine. This is because of high drag generation, which drops the C_L/C_D ratio at lower TSR values, as shown in Figure 9. High drag produces resistance to the motion of the turbine rotor, which generates further fluctuations in aerodynamic forces, especially in the case shown in Figure 10a. High drag and high resistance to motion at lower TSRs are also the main causes of flow separation from the blade surface, producing fluctuations in blade forces. The peak value of aerodynamic

pressure increases with the TSR until it reaches 3.5, and it reduces after that. The higher the aerodynamic pressure, the higher the 'positive' tangential force, which is the ultimate net force moving the blade forward, as stated by Ali et al. [17]. Their study showed that a greater generation of aerodynamic pressure around the turbine blades would produce higher lift, which is converted into positive tangential force (over ninety percent) for moving the blade forward. The tangential force is the positive component of the net force generated by both lift and drag. For the azimuth location, the last quarter (270 to 360°) of the blade's motion is more beneficial for the overall lift and aerodynamic pressure generation, as apparent in Figure 10. This pattern can be observed for all the TSRs with different magnitudes. The results have only been prepared for a single blade at this stage because the rest of the blades seemed to have similar behavior and, therefore, are not presented here.

It can also be noted that, in Figure 10, the magnitude of the shear stress is very small compared to the aerodynamic pressure, which is beneficial for lift generation (as stated above, lift is proportional to pressure, and drag is proportional to shear stress). The peaks of both pressure and shear stress increase with the TSR until it reaches 3.5 (optimum in the present study), and the values begin to drop beyond that point. In all cases, the peak of aerodynamic pressure occurs at almost 360° or 0° (location when the blade is directly in front of the free stream of incoming wind), which is the point of maximum instantaneous lift generation. Moreover, it can be noted that there is negative pressure as well in Figure 10. This negative pressure generates negative lift, which actually opposes the forward motion of the blade. The same was also concluded by Ali et al. [17]. Therefore, it can be stated that not all of the aerodynamic pressure produced is converted into useful lift force.

Figure 11 shows the torque coefficient variation of wind turbine with respect to the azimuth position for all of the three blades. The optimum TSR (3.5) shows the highest peak values of the instantaneous torque coefficient due to high lift at the optimum TSR, as shown in Figure 8. At lower TSRs, the torque coefficient fluctuations are relatively higher as compared to higher TSRs, especially the optimum TSR. These results also reveal the starting characteristics of the wind turbine at different TSRs.

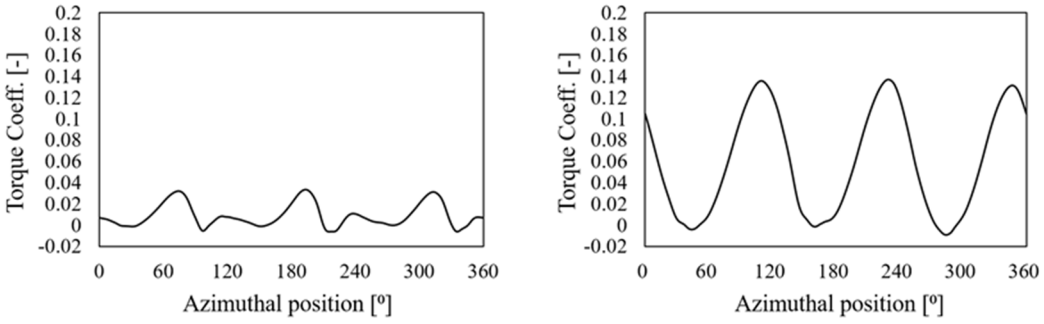

(**a**) (**b**)

Figure 11. *Cont.*

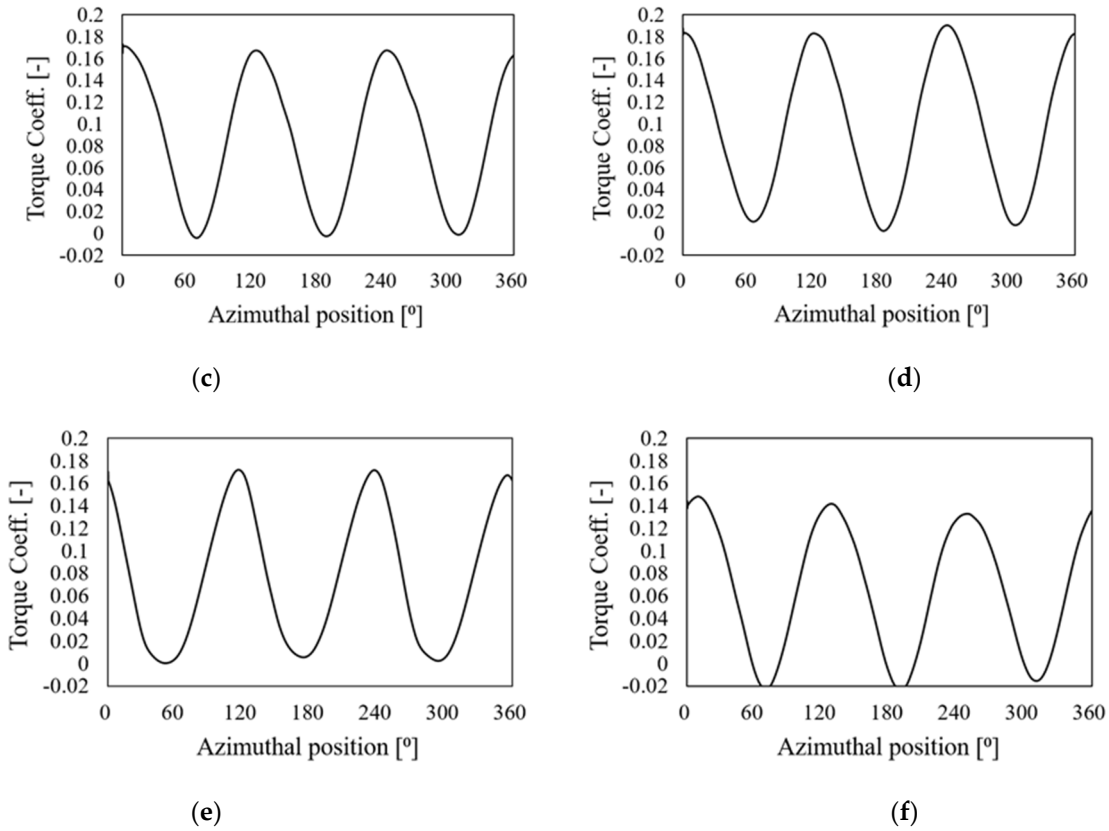

Figure 11. Torque coefficient for one turbine rotor rotation: (**a**) TSR = 1, (**b**) TSR = 2, (**c**) TSR = 3, (**d**) TSR = 3.5, (**e**) TSR = 4, (**f**) TSR = 5.

3.3. Pitch Angle Optimization

One other important aerodynamic parameter is the blade pitch angle (β), defined by the angle between the chord line of the blade and the tangent to the circular rotational path of the blade, as shown in Figure 12. In Figure 12, 'U' is the free-stream wind speed, whereas 'V_t' is the tangential velocity of the rotor blade. The signs of the pitch angle have also been defined accordingly in Figure 12.

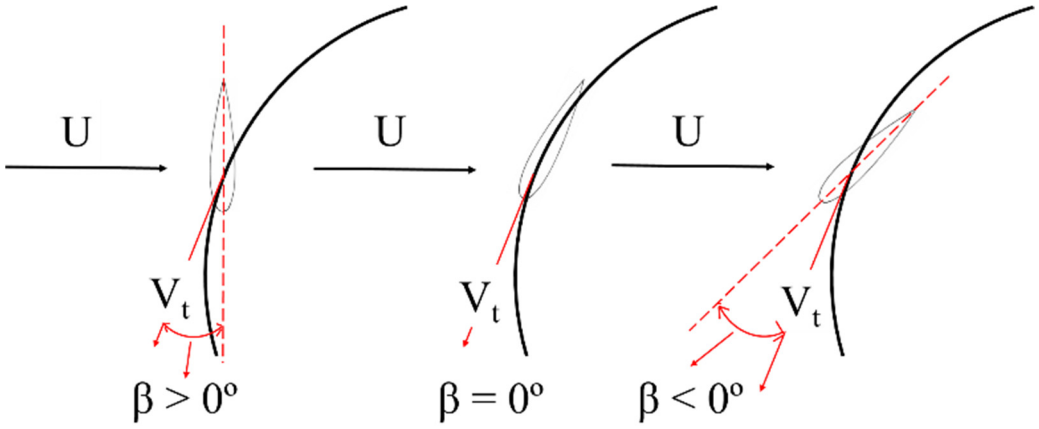

Figure 12. Definition of pitch angle (β).

In the present study, the blade pitch angles are optimized according to the blade rotation at all TSRs, as shown in Figure 13. The blade pitch angles are optimized to ensure that the blade faces the optimum α (as shown in Figure 9) at all times for one blade rotation. This allows the blade to generate maximum stable lift during one blade rotation, which

improves the overall power production process of VAWTs. This is because an optimized pitch angle allows the blade to face the wind to ensure that the angle of attack is constantly optimized, as shown in Figure 9. The optimized pitch and angle of attack will ensure that the blade generates the maximum lift, which will maximize the C_L/C_D ratio. Figure 13 theoretically demonstrates the optimum pitch angle. However, the optimum pitch angle range decreases as the TSR increases, making it 'practically' easier to operate the wind turbine at higher TSRs. In other words, it means that it will require less effort to control the pitch angle of the wind turbine during operation because the change in the pitch angle is small at higher TSRs. This is also one reason that 3.5 is the optimum TSR in the present study, not only because the aerodynamic performance of the wind turbine is superior at this TSR but also it is beneficial from an operational point of view as well.

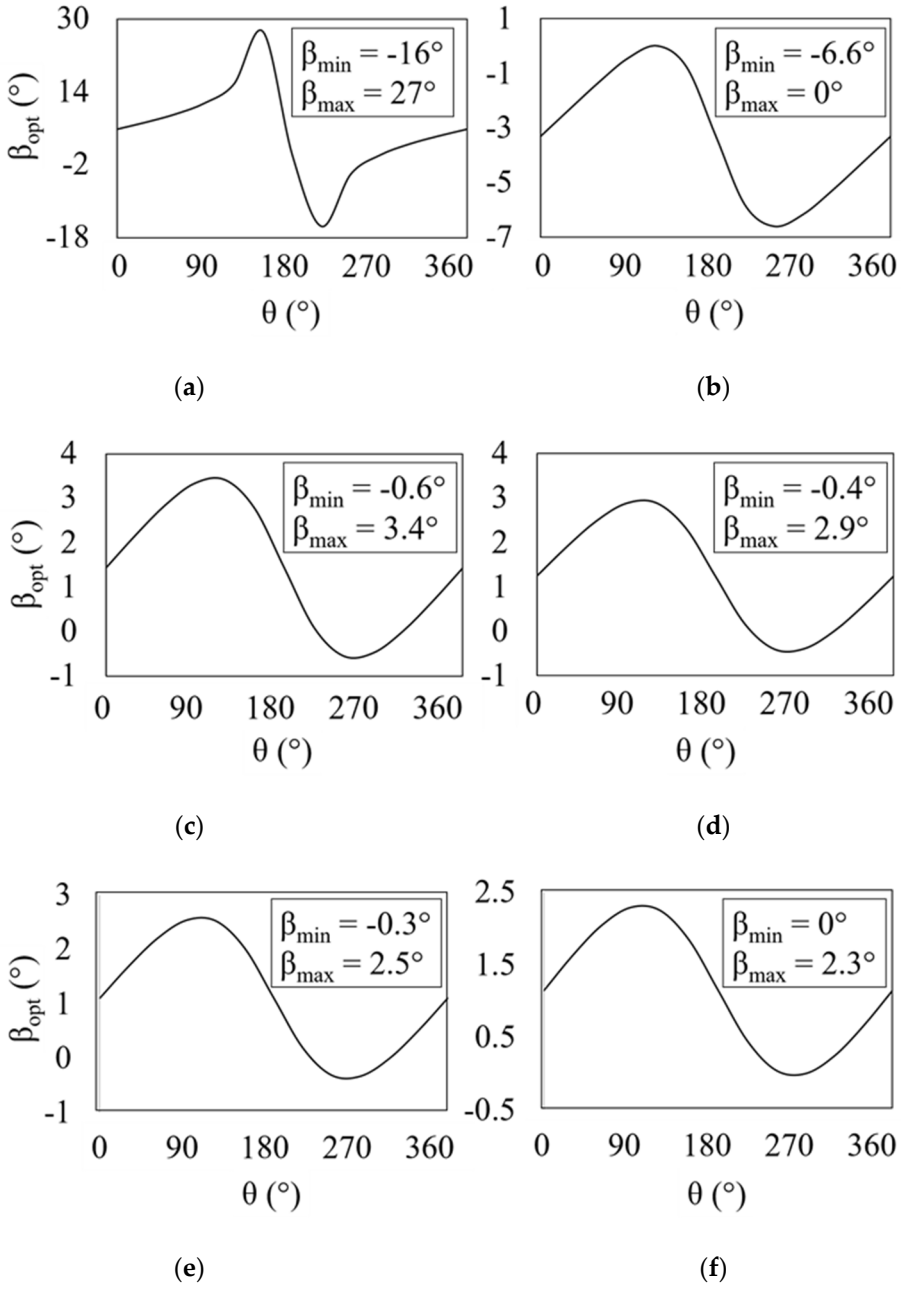

Figure 13. Optimized pitch angle for one turbine rotor rotation: (**a**) TSR = 1, (**b**) TSR = 2, (**c**) TSR = 3, (**d**) TSR = 3.5, (**e**) TSR = 4, (**f**) TSR = 5.

3.4. Internal Flow Analysis

Figure 14 shows the vorticity with respect to the tip speed ratio at the blade rotation angle of zero degrees. At lower tip speed ratios due to high drag and low lift, the flow has more of a chance to separate from the blade surface and generate vortices (TSR = 1) and vice versa for higher TSRs, as shown in Figure 14a. The flow separation is mainly caused by high shear stress, as shown in Figure 10. The vortex and flow separation produce instability in the blade motion, which produces discontinuities in the power production of such turbines. As the flow is not attached to the blade surface due to these vortices, pressure is lost at low TSRs, as shown in Figure 10. However, with an increase in the TSR, the flow has less chances to separate and usually remains in contact with the blade's surface, which helps the blade reduce drag and increase the lift. As shown in Figure 14, the magnitude of vorticity is maximized at lower TSRs (1) and becomes almost identical at higher TSRs (3.5 and 5). It is noted that Figure 14 has been prepared at the same azimuthal position of zero degrees, which is the optimum position of the wind turbine rotor, as concluded from Figure 10.

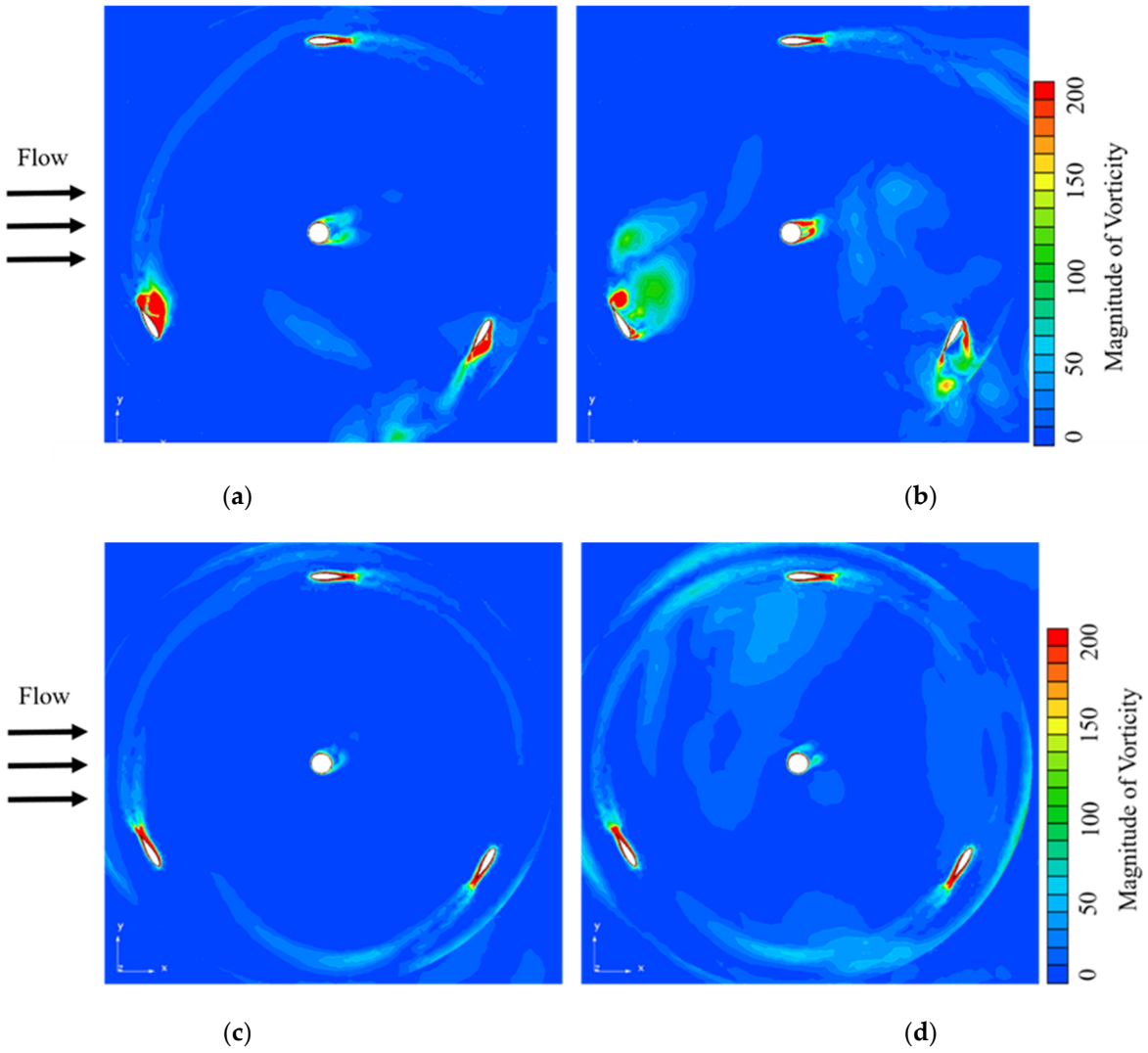

Figure 14. Vorticity with respect to tip speed ratio: (**a**) TSR = 1, (**b**) TSR = 2, (**c**) TSR = 3.5, (**d**) TSR = 5.

Figure 15 shows the vortex formation around a single blade with respect to the TSR. It can be observed that the vorticity reduces from a high value to a lower value as the TSR is increased.

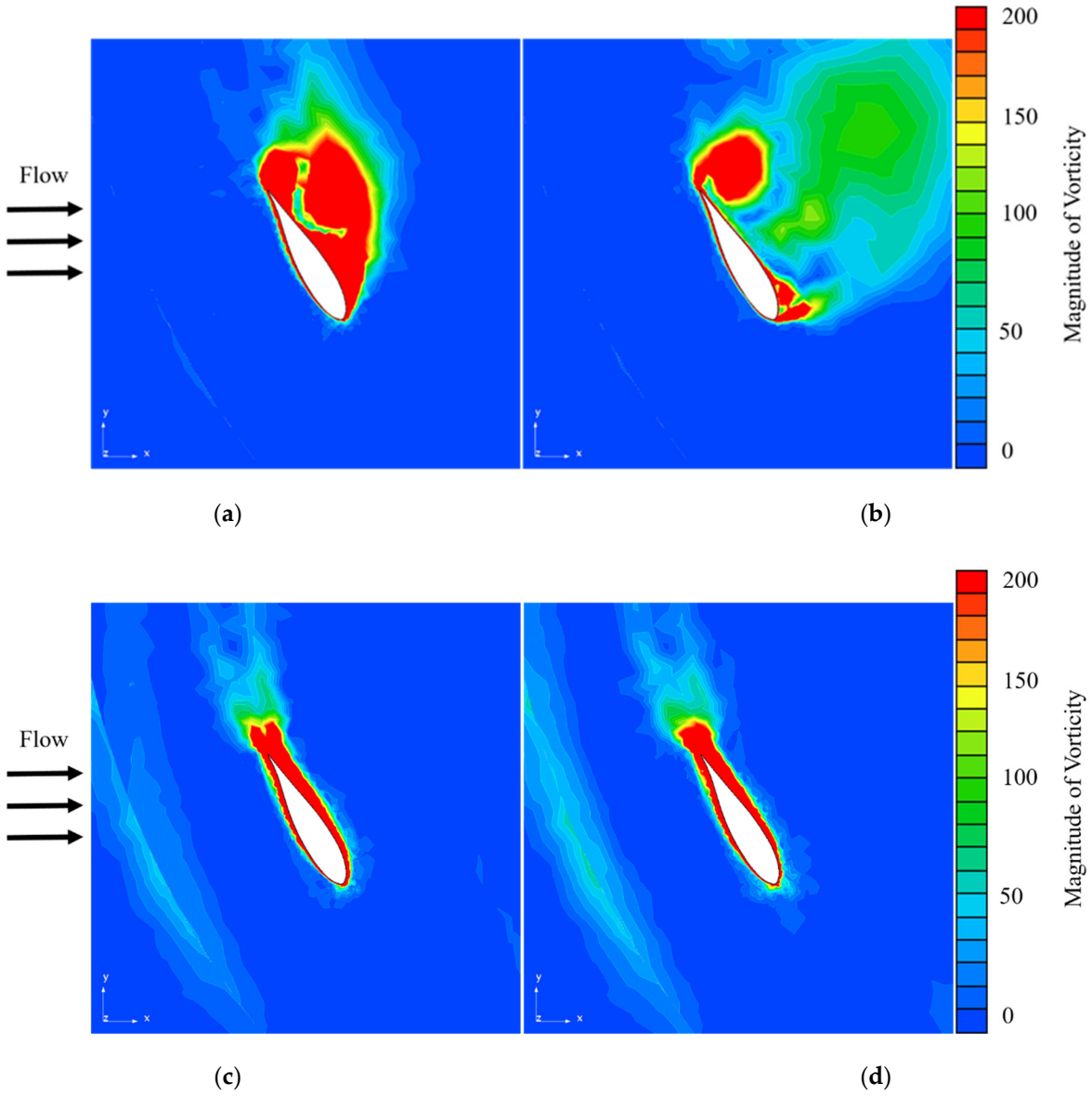

Figure 15. Vorticity around single blade with respect to tip speed ratio: (**a**) TSR = 1, (**b**) TSR = 2, (**c**) TSR = 3.5, (**d**) TSR = 5.

Figure 16 shows the pressure distribution with respect to the blade rotation at a TSR of 3.5. At the blade rotation angle of 45 degrees, there is a very small amount of positive pressure at the blade's leading edge, which grows as the blade rotates. At 110 degrees, there is a relatively significant pressure difference at the leading edge, which generates more lift, and that is subsequently converted into positive tangential force. The buildup of pressure is very smooth and continuous in the case of the optimum TSR (3.5), as shown in Figure 16. The continuous and slow increase in pressure concerning the blade rotation is important for smooth operation and stable torque generation. It is noted that the left side is the pressure side in Figure 16.

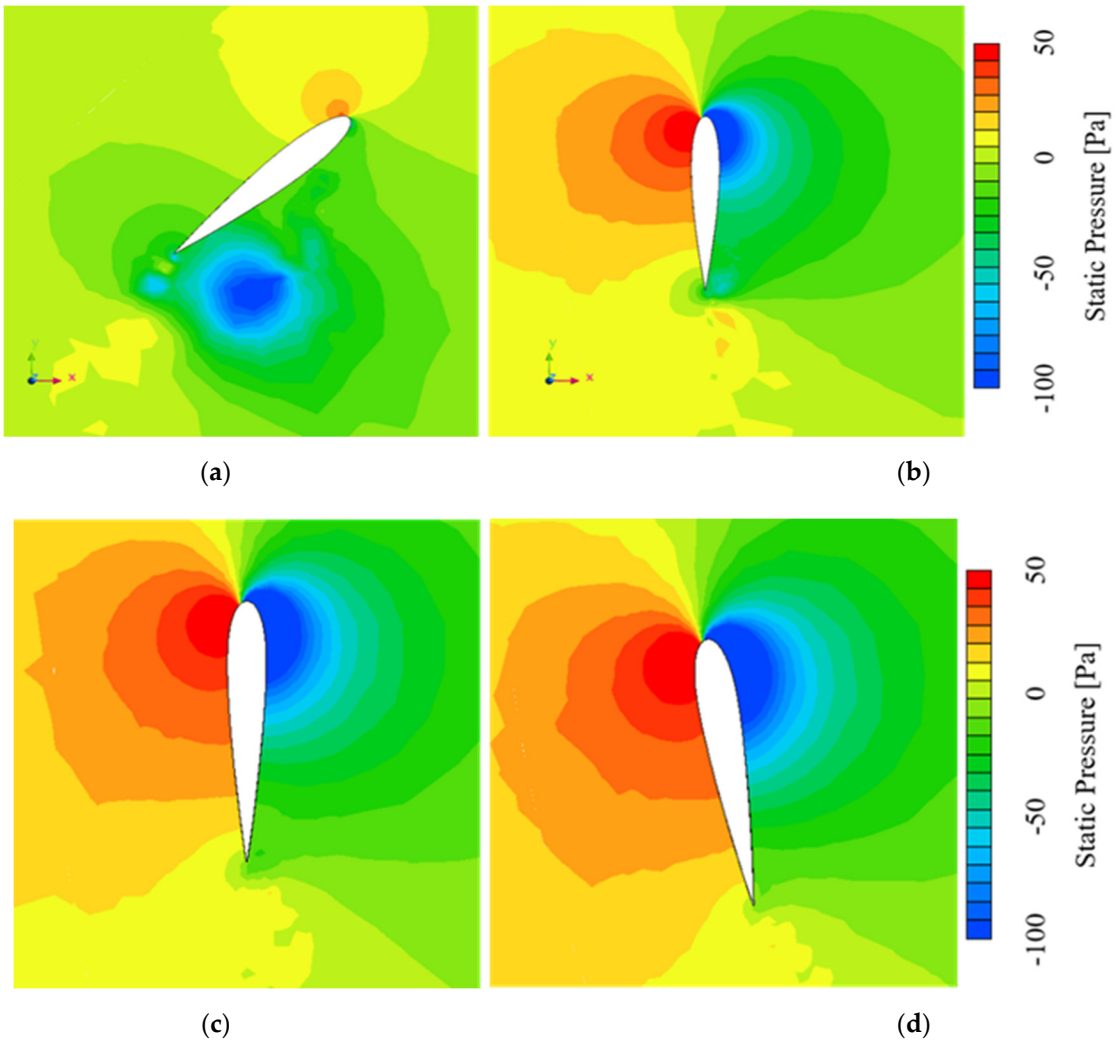

Figure 16. Pressure distribution with respect to the blade rotation at a TSR of 3.5: (**a**) θ = 45°, (**b**) θ = 90°, (**c**) θ = 100°, (**d**) θ = 110°.

4. Conclusions

The present study investigates the conversion of the characteristics of lift and drag forces according to the wind angle of attack at six tip speed ratios (TSRs) for a single blade of an H-Darrieus VAWT having NACA 0015. The study has been conducted using numerical simulations and validated with experimental data. The experimental results are used to validate the numerical model and both types of data, i.e., numerical and experiments, have a margin of error of 10%.

The analysis showed that a TSR of 3.5 is the best-case scenario in the present study, as the ratio between the lift and drag coefficients is maximized at an angle of attack of 5.78°. The TSR and range of the angle of attack are inversely related to each other; as one increases, the other must decrease. However, the maximum lift and drag coefficient ratio at lower TSRs increases almost exponentially and then decreases linearly at higher TSRs. The blade pitch angle has also been optimized at all azimuthal positions in order to maintain a fixed maximum angle of attack. Although the results are presented only theoretically for the optimum pitch angle, modern technology can help to achieve it practically. The two-dimensional colour contours of vorticity at important TSRs show that lower TSRs are not suitable for operating such wind turbines as flow separation destabilizes the rotation of the blade. It produces discontinuities in power production, whereas no such issues are observed at higher TSRs.

Author Contributions: S.A. devised the methodology and wrote the manuscript. C.-M.J. provided his guidance and supervision for this study. All authors have read and agreed to the published version of the manuscript.

Funding: This study was supported with major project funding from the Korea Institute of Civil Engineering and Building Technology. (No. 20200579-001).

Institutional Review Board Statement: Not applicable.

Informed Consent Statement: Not applicable.

Data Availability Statement: Not applicable.

Acknowledgments: We would like to thank CEDIC Co Ltd. Seoul, South Korea for providing their technical support to conduct this research.

Conflicts of Interest: The authors declare no conflict of interest.

Abbreviations

TSR	tip speed ratio
HAWT	horizontal axis wind turbine
LES	large eddy simulation
BC	boundary condition
NACA	national advisory committee for aeronautics
CI	confidence interval
VAWT	vertical axis wind turbine
CFD	computational fluid dynamics
TI	turbulence intensity

References

1. Howell, R.; Qin, N.; Edwards, J.; Durrani, N. Wind tunnel and numerical study of a small vertical axis wind turbine. *Renew. Energy* **2010**, *35*, 412–422. [CrossRef]
2. Claessens, M. The Design and Testing of Airfoils for Application in Small Vertical Axis Wind Turbines. Master's Thesis, Faculty of Aerospace Engineering, Delft, The Netherlands, 2006.
3. Sabaeifard, P.; Razzaghi, H.; Forouzandeh, A. Determination of vertical axis wind turbines optimal configuration through CFD simulations. In Proceedings of the International Conference on Future Environment and Energy, Singapore, 26–28 February 2012; Volume 28.
4. Ponta, F.; Seminara, J.; Otero, A. On the aerodynamics of variable-geometry oval-trajectory Darrieus wind turbines. *Renew. Energy* **2007**, *32*, 35–56. [CrossRef]
5. Yu, J.; Leu, T.; Miau, J.-J. Investigation of reduced frequency and freestream turbulence effects on dynamic stall of a pitching airfoil. *J. Vis.* **2017**, *20*, 31–44. [CrossRef]
6. Mohamed, M. Performance investigation of H-rotor Darrieus turbine with new airfoil shapes. *Energy* **2012**, *47*, 522–530. [CrossRef]
7. Castelli, M.R.; Benini, E. Effect of blade thickness on Darrieus Vertical-Axis Wind turbine performance. In Proceedings of the ICCMS 2011, 3rd International Conference on Computer Modelling and Simulation, Mumbai, India, 7–9 January 2011.
8. Joo, S.; Choi, H.; Lee, J. Aerodynamic characteristics of two-bladed H-Darrieus at various solidities and rotating speeds. *Energy* **2015**, *90*, 439–451. [CrossRef]
9. Gupta, R.; Biswas, A. Computational fluid dynamics analysis of a twisted three-bladed H-Darrieus rotor. *J. Renew. Sustain. Energy* **2010**, *2*, 043111. [CrossRef]
10. Patil, R.; Daróczy, L.; Janiga, G.; Thévenin, D. Large eddy simulation of an H-Darrieus rotor. *Energy* **2018**, *160*, 388–398. [CrossRef]
11. Paraschivoiu, I.; Trifu, O.; Saeed, F. H-Darrieus wind turbine with blade pitch control. *Int. J. Rotating Mach.* **2009**, *2009*, 505343. [CrossRef]
12. Gosselin, R.; Dumas, G.; Boudreau, M. Parametric study of H-Darrieus vertical-axis turbines using URANS simulations. In Proceedings of the 21st Annual Conference of the CFD Society of Canada, Sherbrooke, QC, Canada, 6–9 May 2013; p. 16.
13. Li, Q.A.; Maeda, T.; Kamada, Y.; Murata, J.; Shimizu, K.; Ogasawara, T.; Kasuya, T. Effect of solidity on aerodynamic forces around straight-bladed vertical axis wind turbine by wind tunnel experiments (depending on number of blades). *Renew. Energy* **2016**, *96*, 928–939. [CrossRef]
14. Consul, C.A.; Willden, R.H.J.; Ferrer, E.; McCulloch, M.D. Influence of solidity on the performance of a cross-flow turbine. In Proceedings of the 8th European Wave and Tidal Energy Conference, Uppsala, Sweden, 7–10 September 2009.
15. Chen, B.; Su, S.; Viola, I.M.; Greated, C.A. Numerical investigation of vertical-axis tidal turbines with sinusoidal pitching blades. *Ocean Eng.* **2018**, *155*, 75–87. [CrossRef]

16. Armstrong, S.; Fiedler, A.; Tullis, S. Flow separation on a high Reynolds number, high solidity vertical axis wind turbine with straight and canted blades and canted blades with fences. *Renew. Energy* **2012**, *41*, 13–22. [CrossRef]
17. Ali, S.; Lee, S.M.; Jang, C.M. Effects of instantaneous tangential velocity on the aerodynamic performance of an H-Darrieus wind turbine. *Energy Convers. Manag.* **2018**, *171*, 1322–1338. [CrossRef]
18. Jang, C.M.; Furukawa, M.; Inoue, M. Analysis of Vortical Flow Field in a Propeller Fan by LDV Measurements and LES—Part I: Three-Dimensional Vortical Flow Structures. *Trans. ASME J. Fluids Eng.* **2001**, *123*, 748–754. [CrossRef]